Theor Chem Acc (2004) 111:110–121
DOI 10.1007/s00214-003-0546-z

Theoretical
Chemistry Accounts

Regular article

Theory and computation of electron transfer reorganization energies with continuum and molecular solvent models

I.V. Leontyev[1], **M.V. Basilevsky**[1], **M.D. Newton**[2]

[1] Karpov Institute of Physical Chemistry, ul. Vorontsovo Pole 10, Moscow 105064, Russia
[2] Department of Chemistry, P.O. Box 5000, Brookhaven National Laboratory, Upton, NY 11973, USA

Received: 16 January 2003 / Accepted: 25 May 2003 / Published online: 19 January 2004

Abstract. Contemporary continuum-based models of solvation in polar media are surveyed and assessed, with special focus on non-equilibrium solvation. A new hybrid approach combining molecular-level treatment of inertial solvent response, and inclusion of inertialess solvent response at the continuum level, is presented and illustrated in terms of calculated equilibrium solvation free energies for small molecular ions and reorganization free energies for model dumbbell systems.

Keywords: Solvation models – Electron transfer – Reorganization energy

Introduction

Studies of kinetics and mechanisms of charge transfer reactions in the condensed phase are an important and rapidly developing branch of theoretical chemistry. Electron transfer (ET), the simplest process of this kind, displays the role of solvation effects in chemical kinetics in the purest way. The solvent reorganization accompanying ET mainly contributes to its free energy barrier, and the corresponding reorganization energy is the key kinetic parameter of the ET [1, 2]. Evidently, its computations are a part of the solvation theory. Conventional theoretical approaches are mainly targeted at treating equilibrium solvation effects, whereas solvent reorganization is an essentially non-equilibrium phenomenon. Its study, requiring an extension of standard methodologies, has inspired the elaboration of specific new algorithms.

Earlier theoretical formulations of the ET rate expression [3, 4] were based on the extremely simple homogeneous solvent model, neglecting the excluded volume effect. Appearance of a new generation of continuum solvent models, among which the PCM [5, 6, 7] is one of the most efficient and popular, prompted remarkable progress in studies of solvation equilibria. For the implementation to ET reaction kinetics, a development of the existing prescriptions proved to be necessary [8, 9, 10]. Successful computations of ET reorganization energies became possible only by means of a more sophisticated solvent model, beyond the PCM [11, 12]. Further progress, especially in the field of biological applications, requires recent molecular solvent models to be invoked as fundamental background to the ET theory.

In the present paper we outline the basic principles underlying the theoretical treatment of ET reorganization energies, and briefly discuss several computational procedures, including the most contemporary. The methodology is still at the development stage, and refined versions are expected to appear in the near future.

General formulations

The linear response approach in the functional space

Two basic field variables underlying the solvation theory are solute charge density $\rho(r)$ and medium response field $\Phi_{eq}(r)$. They can be considered, respectively, as generalized collective solute and solvent coordinates. Being both functions of space point vector r, they actually represent an infinite number (a three-dimensional continuum) of variables. The following general relations can be established [13]. The linear response postulates a linear connection between a given field $\rho(r)$ and a field $\Phi_{eq}(r)$ that is equilibrated to $\rho(r)$:

$$\Phi_{eq}(r) = \int d^3r' K(r,r')\rho(r') \equiv \hat{K}\rho(r) \tag{1}$$

The two-point function $K(r,r')$ is called the integral kernel (or Green's function); it is symmetric: $K(r,r') = K(r',r)$. The second part of Eq. 1 reformulates the theory in terms of the linear symmetric operator $\hat{K}$ (Green's operator) represented by kernel $K(r,r')$. Eq. 1

Contribution to the Jacopo Tomasi Honorary Issue

Correspondence to: M.V. Basilevsky
e-mail: basil@cc.nifhi.ac.ru

corresponds to a pure linear case; its generalization is considered below.

A conventional approximation of the ET theory considers free energy surfaces as a superposition of two shifted paraboloids, the quadratic functions of solvent coordinates. For the present case we introduce the quadratic free energy functional (FEF) $\Delta F[\Phi|\rho]$, or for brevity, $\Delta F[\Phi]$:

$$\Delta F[\Phi] = C + \int d^3r \rho(r)\Phi(r) + \frac{1}{2}\int d^3r d^3r' L(r,r')\Phi(r)\Phi(r') \tag{2}$$

The first constant term is Φ-independent. The second term, representing the solute/solvent interaction, is linear in Φ. The third quadratic term is called "the solvent self-energy". Its kernel $L(r,r') = L(r',r)$ is symmetric. A purely linear case is the simplest and most obvious; then the constant C and the kernel L in the self-energy are ρ-independent.

One can define the linear symmetric integral operator $\hat{L}$, with kernel $L(r,r')$, similar to operator $\hat{K}$ in Eq. 1. Using this contracted notation, the basic relation between $\hat{K}$ and $\hat{L}$ is established by a variation of FEF (2) relative to Φ:

$$\hat{K} = -\hat{L}^{-1} \tag{3}$$

For a stable system $\hat{L}$ is positive-definite and $\hat{K}$ is negative-definite.

Given solute charge density $\rho(r)$, Eqs. 1 and 3 determine the minimum point $\Phi = \Phi_{eq}$ of FEF(2). The corresponding equilibrium solvation free energy is

$$\begin{aligned} \Delta F_{eq} &= C + \tfrac{1}{2}\langle\rho|\hat{K}|\rho\rangle \\ \langle\rho|\hat{K}|\rho\rangle &= \int d^3r d^3r' K(r,r')\rho(r)\rho(r') \end{aligned} \tag{4}$$

Purely electrostatic interactions have been considered above. In real life they always coexist with van der Waals interactions. The interference of electrostatic and van der Waals forces results in the observation [14, 15, 16] that $\Phi_{eq} \neq 0$ when $\rho = 0$. This fact can be taken into account by a slight modification of the above theory. Equations 1 and 2 must be generalized by introducing a constant (nonvarying) field Φ_0 and making the change $\Phi \to \Phi' = \Phi - \Phi_0$. By this means, from Eq. 1 one immediately obtains:

$$\Phi_{eq}(r) = \Phi_0 \quad (\rho = 0) \tag{5}$$

Further analysis is simplified if kernel $K(r,r')$ (and, therefore, kernel $L(r,r')$) is ρ-independent. The consistency of the above formulation then requires that constant term C in the FEF (1) is also ρ-independent. According to Eq. 4, $\Delta F_{eq} = C$ corresponds to the case $\rho = 0$ and C can be interpreted as van der Waals free energy, whereas the last term in Eq. 2 represents a complementary self-energy term, associated with pure electrostatic effects (it vanishes at equilibrium point (5)).

We can now consider two levels for treating nonlinear effects. The ρ-dependence of Φ-independent parameters appearing in Eqs. 1 and 2 is introduced as a first step. We allow for a ρ-dependence of constant C, kernels $L(r,r')$ and $K(r,r')$ and the field shift, denoted as $\bar{\Phi}\left(\lim_{\rho\to 0}\bar{\Phi} = \Phi_0\right)$. In this way, the generalized linear theory is based on the equation

$$\Delta F[\Phi|\rho] = C + \int d^3r \rho(\Phi - \bar{\Phi}) + \frac{1}{2}\int d^3r d^3r' (\Phi - \bar{\Phi})L(r,r')(\Phi - \bar{\Phi}) \tag{6}$$

Here C, L and $\bar{\Phi}$ depend on ρ. In this way the quadratic dependence of the FEF relative to the response field Φ is retained. It is this parabolic dependence on the solvent coordinate that constitutes the essence of the ET theory. On the other hand, the counterpart of Eqs. 1 and 3,

$$(\Phi_{eq} - \bar{\Phi}) = \hat{K}\rho; \quad \hat{K} = -L^{-1}; \tag{7}$$

represents a nonlinear theory.

However, we can still treat deviations of the solvent coordinate from its equilibrium position in terms of a linear model. The corresponding FEF representation

$$\Delta F[\Phi|\rho] = \Delta F_{eq} + \frac{1}{2}\langle\Phi - \Phi_{eq}|\hat{L}|\Phi - \Phi_{eq}\rangle \tag{8}$$

serves as a basis for a linear (relative to Φ) theory of nonequilibrium solvation effects, such as reorganization energy. Note that the linearized expression (4) for the equilibrium solvation free energy is no longer valid. The value ΔF_{eq} can be obtained from Eq. 7 by thermodynamic integration [13].

A concluding remark is in order. Although $\Phi(r)$ is a continuum field, it is well-defined for both continuum and molecular solvent models, and serves equally well as a collective solvent coordinate in both cases. This is the main advantage of the present formulation. It suggests a unified treatment which implies only that different (continuum or molecular) solvent models generate different forms for kernels $L(r,r')$ and $K(r,r')$. In other respects the structure of linear continuum and molecular theories is the same. We also note that a continuum theory based on the Maxwell equations is fully linear and no ρ-dependencies should be considered. However, this complication becomes evident when molecular solvent models are addressed.

The reorganization energy

We now consider two charge distributions $\rho_I(r)$ and $\rho_{II}(r)$ corresponding to the initial and final states of a ET process. The relevant equilibrium response fields $\Phi_I(r)$ and $\Phi_{II}(r)$ are:

$$\Phi_I = \hat{K}_I\rho_I; \quad \Phi_{II} = \hat{K}_{II}\rho_{II} \tag{9}$$

Operator $\hat{K}$ can be ρ-dependent, which explains the state indices I and II labelling $\hat{K}$ in Eq. 9. The conventional (truly linear) theory neglects this ρ-dependence by assuming $\hat{K}_I = \hat{K}_{II} = \hat{K}$.

In the general case we can find equilibrium free energies ΔF_I and ΔF_{II}, (corresponding to charges ρ_I and ρ_{II}) by thermodynamic integration. According to general equation (8),

$$\begin{aligned} \Delta F[\Phi|\rho_I] &= \Delta F_I - \tfrac{1}{2}\langle\Phi - \Phi_I|\hat{K}_I^{-1}|\Phi - \Phi_I\rangle \\ \Delta F[\Phi|\rho_{II}] &= \Delta F_{II} - \tfrac{1}{2}\langle\Phi - \Phi_{II}|\hat{K}_{II}^{-1}|\Phi - \Phi_{II}\rangle \end{aligned} \tag{10}$$

We recall that operators $\hat{K}_I$ and $\hat{K}_{II}$ are negative-definite. We also note that, although field shifts $\bar{\Phi}$ are not explicitly included in the free energy expressions for the sake of brevity, Eq. 10 does account for the shift effect. Provided $\bar{\Phi}$ is ρ-independent it cancels in the field differences $\Phi - \bar{\Phi}_I$ and $\Phi - \bar{\Phi}_{II}$. The free energy surface formed by the pair of paraboloids (10) is shown schematically in Fig. 1. This figure illustrates how two reorganization energies λ_I and λ_{II} arise by inserting $\Phi = \Phi_{II}$ in the first line of Eq. 10 and $\Phi = \Phi_I$ in its second line:

$$\begin{aligned} \lambda_I &= -\tfrac{1}{2}\langle\Phi_{II} - \Phi_I|\hat{K}_I^{-1}|\Phi_{II} - \Phi_I\rangle \\ \lambda_{II} &= -\tfrac{1}{2}\langle\Phi_I - \Phi_{II}|\hat{K}_{II}^{-1}|\Phi_I - \Phi_{II}\rangle \end{aligned} \tag{11}$$

They become equal ($\lambda_I = \lambda_{II} = \lambda$) in the case $\hat{K}_I = \hat{K}_{II} = \hat{K}$ when operator $\hat{K}$ becomes ρ-independent. Then the standard Marcus expression for ET energy barrier ΔU arises:

$$\begin{aligned} \Delta U &= \tfrac{(\Delta\Delta F + \lambda)^2}{4\lambda} \\ \Delta\Delta F &= \Delta F_{II} - \Delta F_I \end{aligned} \tag{12}$$

A more complicated expression arises in case (11). If λ_I and λ_{II} are close ($\left|\frac{\lambda_{II} - \lambda_I}{\lambda_I}\right| \ll 1$), the average reorganization energy $\lambda = (\lambda_I + \lambda_{II})/2$ can be inserted into Eq. 12 as a reasonable approximation.

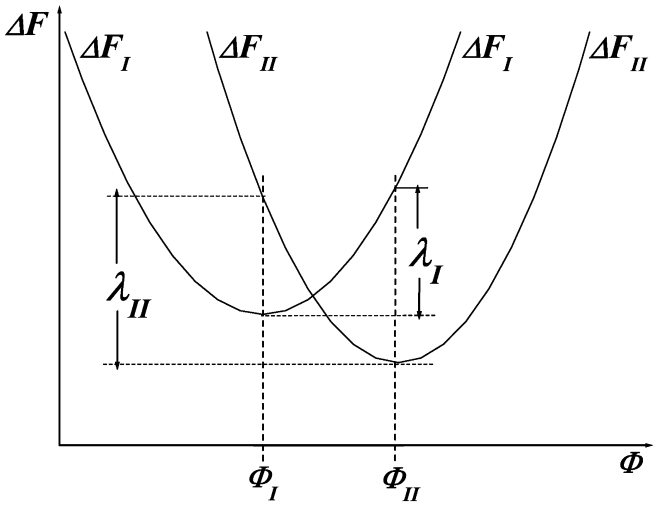

Fig. 1. Schematic one-dimensional illustration of free energy changes in a charge transfer reaction in the two-state representation. The two parabolic energy curves represent FEFs for initial ($\rho = \rho_{\mathrm{I}}$) and final ($\rho = \rho_{\mathrm{II}}$) states in the harmonic approximation

Let us now return to the conventional case with the ρ-independent response operator $\hat{K}$. Then Eqs. 11 reduce to

$$\lambda = \frac{1}{2}(T_{\mathrm{I\,I}} + T_{\mathrm{II\,II}} - 2T_{\mathrm{I\,II}}) \tag{13}$$

Here T_{ab} are the elements of the so called reorganization matrix:

$$T_{ab} = -\int d^3 r \rho_a(r)\Phi_b(r) = -\langle \rho_a|\hat{K}|\rho_b\rangle \tag{14}$$

where the contracted notation for the integral follows Eq. 4.

Equation 13 acquires the structure of the well-known two-sphere expression for the reorganization energy [4, 17] by defining two effective sphere radii, $R_{\mathrm{I\,I}}$ and $R_{\mathrm{II\ \ II}}$, proportional to $\frac{1}{T_{\mathrm{I\,I}}}$ and $\frac{1}{T_{\mathrm{II\,II}}}$, and the effective sphere separation $R_{\mathrm{I\,II}}$, proportional to $\frac{1}{T_{\mathrm{I\,II}}}$. This interpretation makes sense when the two ET states (donor state I and acceptor state II) are well-localized and the donor and acceptor spheres don't overlap significantly. Equation 13 remains valid in all continuum theories when the ρ-dependence of operator $\hat{K}$ does not appear.

Continuum theories of ET

The PCM approach

In the early stages of the development of ET theory, the simplest continuum models were used [4, 18]. As a rule, excluded volume of the solute ET system was neglected and spherical shapes of donor and acceptor centers were postulated. Such approximations become too restrictive when ET in real chemical objects was studied. They can be circumvented in terms of the PCM methodology [5, 6, 7], which is widely accepted for computations of equilibrium solvation effects. Its application to treating non-equilibrium phenomena, such as reorganization energies, is based on the linear theory outlined briefly above. Within a PCM realization, the response operator $\hat{K}$ is defined by the following pair of equations:

$$\begin{aligned} &\sigma(r) = \tfrac{1}{4\pi}\left(1 - \tfrac{1}{\varepsilon_0}\right)\left[\hat{V}\rho(r) + \hat{S}\sigma(r) + 2\pi\sigma\right],\ r \in \textstyle\sum \\ &\Phi(r) = \int\limits_{\Sigma} d^2 r' \tfrac{\sigma(r')}{|r-r'|},\ r \in V_0 \end{aligned} \tag{15}$$

Here $\hat{V}$ and $\hat{S}$ are volume and surface integral operators:

$$\begin{aligned} &\hat{V}\rho(r) = \int\limits_{V_0} d^3 r' a(r,r')\rho(r') \\ &\hat{S}\sigma(r) = \int\limits_{\Sigma} d^2 r' a(r,r')\sigma(r') \\ &a(r,r') = \tfrac{\partial}{\partial n(r)}\tfrac{1}{|r-r'|} \end{aligned} \tag{16}$$

The cavity surrounding the solute particle is constructed using the PCM prescriptions [5, 6, 7]. The dielectric constant $\varepsilon = 1$ inside the cavity and $\varepsilon = \varepsilon_0$ (the static permittivity) outside the cavity. The cavity boundary Σ surrounds the solute volume V_0; V_1 is the external volume. This well-known scheme is illustrated in Fig. 2a. The response field is determined in terms of the surface charge density $\sigma(r)$ on the cavity boundary. The first equation (15) is the integral equation [19, 20] defining $\sigma(r)$, given solute charge density $\rho(r)$. The kernel $a(r,r')$ in Eq. 16 is obtained by performing the normal derivative $\partial/\partial n(r)$ on the boundary surface Σ; the symbol r in braces means that the differential of variable r is considered.

Equations 15 and 16 represent a purely linear algorithm implicitly defining the operator $\hat{K}$. Here, as in any other continuum theory, $\hat{K}$ does not depend on ρ. Although explicit evaluation of $\hat{K}$ is unavailable, its matrix elements $\langle \rho_a|\hat{K}|\rho_b\rangle$ with different solute distributions ρ_a, ρ_b can be calculated. According to Eq. 14 these matrix elements comprise the reorganization matrix, opening the door to the PCM evaluation of reorganization energy λ.

One more complication should be mentioned here. The response field $\Phi(r)$ actually contains two components: the fast inertialess field $\Phi_\infty(r)$ and the sluggish inertial field $\Phi_{\mathrm{in}}(r)$. The first term is associated with electronic polarization of the medium by the solute charge. The second one represents orientational and translational solvent polarization modes. These modes involve charge distributions of solvent particles, both permanent and those induced by the environment (note that the charges induced by the solute create Φ_∞). Altogether, $\Phi = \Phi_{\mathrm{total}}$, such that within a linear response approximation:

$$\Phi_{\mathrm{total}}(r) = \Phi_\infty(r) + \Phi_{\mathrm{in}}(r) \tag{17}$$

Only the inertial field contributes to the ET reorganization energy [1–3]. It can be separated from the total response by making two PCM computations. Performing the first computation with $\varepsilon = \varepsilon_0$ outside the cavity provides $\Phi_{\mathrm{total}}(r)$. This procedure implicitly defines the total response operator $\hat{K}_{\mathrm{total}}$. The second computation

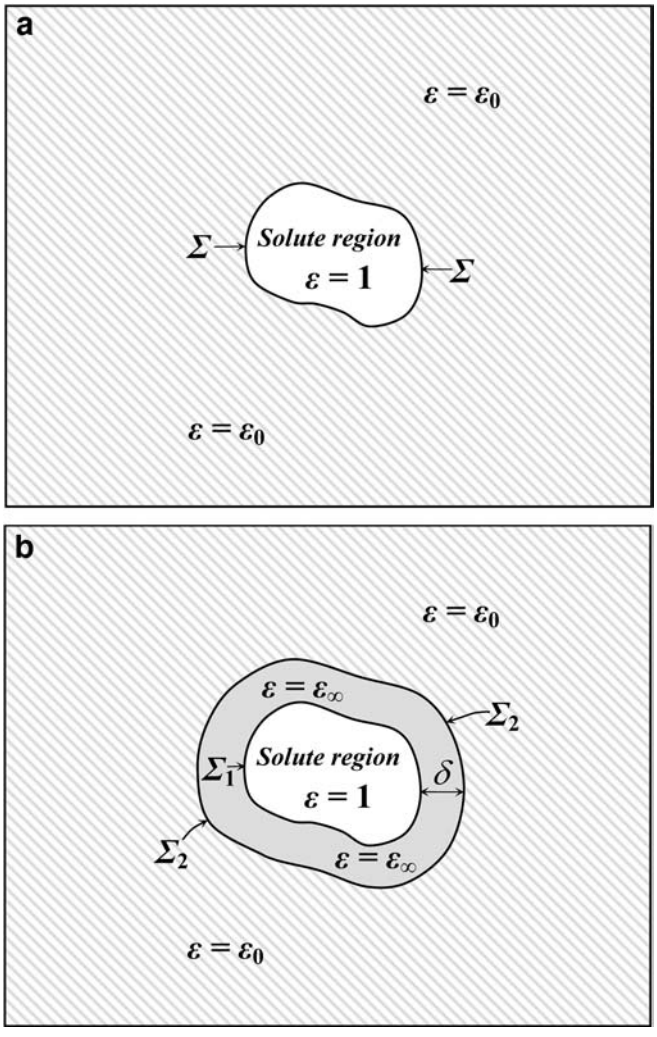

Fig. 2. Schemes of continuum solvent models. The solute charge density is confined within the solute region V_0. **a** PCM; **b** FRCM

is performed using $\varepsilon = \varepsilon_\infty$ (the optical permittivity) outside the cavity. It gives Φ_∞ and, implicitly, the inertialess response operator $\hat{K}_\infty$. The required inertial component arises as differences:

$$\Phi_{\text{in}} = \Phi_{\text{total}} - \Phi_\infty$$
$$\hat{K}_{\text{in}} = \hat{K}_{\text{total}} - \hat{K}_\infty \qquad (18)$$

These quantities should be inserted instead of Φ and $\hat{K}$ in the procedure formulated in an earlier section (''The reorganization energy'').

As described in this section on the reorganization energy, computations of reorganization energies are based on the solute charge densities $\rho_a(r)$ obtained in gas phase SCF or CI computations (usually, SCF or 2×2 CI is sufficient). An alternative method, based on SCRF computations of $\rho_a(r)$, has also been tested and implemented [8, 9, 10]. This modification accounts for electronic polarization of the solute by the solvent response field. The results of the two approaches are quite similar. The following discussion of continuum level results is based on computations using nonlinear SCRF versions of PCM and its advanced modification considered below. The simpler fully linear CI approach is combined with molecular level studies in a later section (''Molecular level solvent models'').

Implementing these techniques, test computations with model ET substrates $(CH_2)_n^+$ and $(CH_2)_n^-$ in water solvent have been performed, first with semi-empirical [8] and then with ab initio [9] charge distributions $\rho(r)$. Their extension to real ET systems [10] has revealed a strong discrepancy between computed and experimental solvent reorganization energies. Successful computations are possible only via a more sophisticated technique described below. Nonetheless, several PCM-type computations of reorganization energies have been reported since [21, 22].

Breakdown of the PCM approach and the advanced continuum theory

Solvent reorganization energies for a series of intramolecular ET reactions have been studied experimentally [23, 24, 25]. The ET solute systems were specially synthesized, and were selected in order to eliminate ambiguities in the interpretation of experimental data as much as possible. A typical illustration is suggested in Fig. 3. The choice of rigid bridge structures fixed almost definitely the relative distance between the donor (biphenylyl) and acceptor (naphtyl) centers and their mutual orientation. Some remaining ambiguity due to internal rotations of naphthyl and phenyl groups can be eliminated by a quantum-chemical computation of most stable conformational structures.

Computed λ values for systems shown in Fig. 3 are compared with the experiment in Table 1. The PCM computation seems to systematically exaggerate the solvent reorganization energies, a problem deserving special consideration.

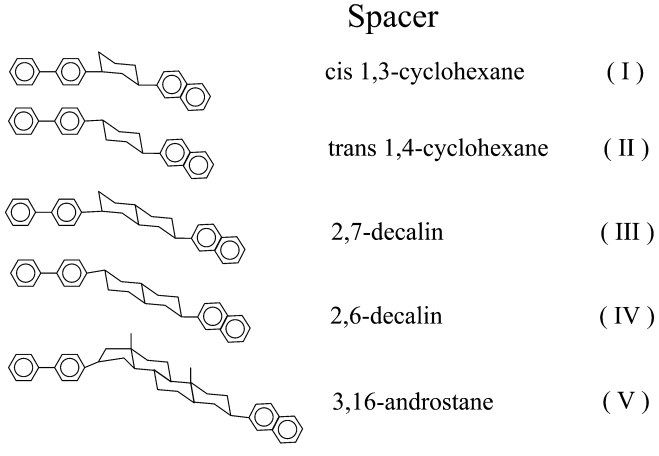

Fig. 3. Typical intramolecular ET systems. Charge is transferred from the biphenylyl to the naphthyl fragment through the spacer structure

Table 1. Solvent reorganization energies for intramolecular charge transfer in systems shown in Fig. 3

ET system[a]		PCM results[b,c] (eV)	FRCM results[b,c] (eV)	Experimental[d] (eV)
I	−	1.07	0.41	0.39
	+	1.02	0.42	0.41
II	−	1.16	0.45	0.47
	+	1.09	0.46	0.49
III	−	1.20	0.50	0.50
	+	1.14	0.51	0.52
IV	−	1.25	0.53	0.55
	+	1.18	0.55	0.57
V	−	1.34	0.61	0.62
	+	1.27	0.63	0.64

[a] Structure numbers correspond to Fig. 3. Symbols "−" and "+" refer to anionic and cationic systems respectively (in other words electron and hole transfer);
[b] solvent as tetrahydrofuran, $\delta = 2.3$ Å in Eq. 20, see [11, 12];
[c] the SCRF version;
[d] the experimental estimates are based on measured values $\lambda = 0.62 \pm 0.03$ (electron transfer) and $\lambda = 0.64 \pm 0.03$ (hole transfer) for the largest structure V [23,24]. Figures for smaller structures were obtained by means of an interpolation procedure based on the Marcus analog of Eq. 13: $\lambda = \frac{1}{2}\left(\frac{1}{\varepsilon_\infty} - \frac{1}{\varepsilon_0}\right)\left(\frac{1}{R_D} + \frac{1}{R_A} - 2\frac{1}{R_{DA}}\right)$, where R_D and R_A are effective radii of donor and acceptor centers (interpolation parameters) respectively, and R_{DA} is the donor-acceptor separation (measured using the geometry of a given structure)

A comment on the strategy of PCM computations [5, 6, 7] is required at this point. The theory is, of course, semi-empirical, based on the adjustable cavity parameterization. The cavity, assembled as a collection of overlapping atomic spheres drawn around each solute atom, has a boundary formed by external fragments of these spheres. The basic PCM parameter is the ratio κ between electrostatic (r_{el}) and van der Waals (r_{vdW}) atomic radii.

$$\kappa = \frac{r_{el}}{r_{vdW}} \tag{19}$$

It is assumed to be the same for all atoms, and indeed proved to be approximately constant for many different solvents [7, 26].

The choice (19) is inferred from numerous computations of equilibrium solvation free energies. It leaves no flexibility to adjust computations of non-equilibrium solvation phenomena, such as reorganization energies. The poor computational results seen in Table 1 point to internal inconsistency in the theory, which could not be revealed when only equilibrium effects were considered. Similar results were observed in computations for other ET systems.

This inconsistency has been eliminated using the so-called frequency resolved cavity model (FRCM) [11, 12, 27]. This method differs from the PCM method because it separates the inertialess (high-frequency) response of the medium from the inertial (low-frequency) one. The solute is surrounded by two surfaces (Σ_1 and Σ_2), as shown in Fig. 2b, each of which is constructed as a collection of overlapping spheres similar to the PCM model. For the first cavity, contained within the internal surface Σ_1, the radius of each sphere is defined as $r_1 = \kappa r_{vdW}$, where $\kappa = 0.9$ is a universal empirical factor common to all solvents and r_{vdW} is the van der Waals radius of the particular solute atom. The radius r_2 defining the external surface is given by

$$r_2 = r_1 + \delta = 0.9 r_{vdW} + \delta \tag{20}$$

where δ is another empirical constant, pertaining to the given solvent (it correlates roughly with the characteristic size of a solvent particle). Between the two surfaces the medium is represented by the inertialess dielectric constant ε_∞, while outside the outer cavity the static dielectric constant ε_0 is applied. The layer between the surfaces corresponds roughly to the first solvation shell. Calculation of the potential field $\Phi(r)$ in this scheme amounts to simultaneously solving two coupled PCM-type equations describing charge densities on the surfaces of two cavities, namely σ_1 (on the inner surface) and σ_2 (on the outer one); they contribute additively to the total $\Phi(r)$ and are similar to Eq. 15.

A simple illustration of this approach is a spherically symmetric Born-like case (a point ion of charge Q placed at the center of two concentric spheres with radii r_1 and r_2). Its total solvation energy

$$\Delta F_{eq} = -\frac{Q^2}{2}\left[\left(1 - \frac{1}{\varepsilon_\infty}\right)\frac{1}{r_1} + \left(\frac{1}{\varepsilon_\infty} - \frac{1}{\varepsilon_0}\right)\frac{1}{r_2}\right] \tag{21}$$

is naturally divided into inertialess and inertial contributions; it reduces to the Born expression when $r_1 = r_2$. The extra cavity parameter, namely the width δ of the intersurface layer in Eq. 20, brings additional flexibility and allows us to simultaneously account for both equilibrium solvation energies and the non-equilibrium ET reorganization energies.

The FRCM results corresponding to the choice of cavity parameters following Eq. 20, with $\delta = 2.3$ Å for tetrahydrofuran, are compared with PCM ones in Table 1. They fit the observed (or interpolated) λ values reasonably well. Other examples of a successful FRCM treatment have been also reported [11, 12, 27]. We don't discuss here different, more or less sophisticated, versions of λ computations (extended CI/SCRF taking into account the solute polarizability, different methods for orbital SCF computations, and so on). The basic results illustrated by Table 1 are not sensitive to such computational details. Altogether they demonstrate serious problems arising in a conventional continuum solvent theory, which are resolved by its FRCM modification.

Inherent problems of the continuum approach

Several observations cannot be properly accounted for in the framework of continuum electrostatic solvent

models. The most remarkable example is the temperature dependence of reorganization energies. In a standard continuum (say, PCM or FRCM) computation it emerges via the temperature dependence of the dielectric permittivity ε_∞ and ε_0. This description proves to be ineffective. It not only strongly underrates the magnitude of the effect, but also predicts its sign incorrectly. The value of λ decreases with the increase in the temperature [28, 29] whereas its estimate based on the temperature change of ε_∞ and ε_0 suggests the opposite trend. The origin of this failure lies in the fact that the temperature dependence of the solute cavity parameters is ignored. The size and the shape of the cavity are fixed in a continuum computation and no solid prescription is known for incorporating their changes. This can only be done empirically, so the temperature trend of λ was reproduced in terms of the FRCM by properly fitting the cavity parameter δ (see Eq. 20) [27].

The continuum approach, in its local electrostatic version, is also unable to explain significant values (0.1–0.2 eV) of reorganization energies observed in nonpolar solvents (benzene, dioxane) [30] where $\varepsilon_0 = \varepsilon_\infty$ and a computation shows no effect.

At the fundamental level of description, the effects missing in the continuum solvent models are associated with the translational diffusive motion of solvent particles [31, 32, 33, 34, 35]. It coexists with orientational motion of solvent dipoles that was traditionally accepted [1, 2, 3, 4] to be the main origin of solvent polarization. On the other hand, quadrupolar and higher multipolar moments can be also considered in terms of a sophisticated refined continuum theory [36, 37, 38]. Both types of effects missing in traditional continuum formulations were described in terms of a simple molecular level model (mean spherical approximation or MSA [39, 40, 41]) based on a spherical approximation for shapes of solute and solvent particles [42, 43]. It proved to be efficient in describing changes of ET parameters for a single solute in a number of solvents with varying polarity [44, 45].

A nonlocal electrostatic theory [46, 47] is a conventional way to bring elements of internal solvent structure into a continuum solvent treatment. In the static case, the dielectric function $\varepsilon(k)$ of wave vector k carries all of the information about the solvent structure. In the simplest Lorentzian parameterization of $\varepsilon(k)$, the parameter l, called "the correlation length", characterizes the size of solvent particles. For a spherical ion of radius r_0 the expression for solvation energy is available with an approximate [46, 47] or complete [48] accounting of the excluded volume effect. The ratio l/r_0, a measure of characteristic sizes of solvent and solute particles, governs the significance of effects of solvent structure. This ratio also appears naturally in the MSA, the simplest true molecular theory.

The Lorentzian permittivity model fails to account completely for dielectric response in real solvents. Being transformed to coordinate space this function generates a purely exponential decay of screening effects. Numerical simulations [49, 50, 51, 52, 53, 54] have revealed a pole structure of $\varepsilon(k)$ generating oscillations of the permittivity kernel and resulting response fields in coordinate space. In an accurate simulation of water [55] a Lorentzian peak was observed for small k values and it was suppressed by pole singularities when k increased. This complicated behavior, combining both decay and oscillation effects, is caused by the interference of density and polarization fluctuations of molecular solvent dipoles [56]. At a qualitative level, the simple Lorentzian model with several correlation lengths [47] remains a useful approximation. It can serve as a phenomenological counterpart of simplistic molecular models, like MSA.

The MSA also proved to be successful for treating the temperature dependence of reorganization energies [28, 29]. Here the solute radius depends on temperature explicitly. The same result could be obtained by introducing the temperature dependence of the correlation length l of non-local theories. However, in both cases the spherical solute model is a quite undesirable limitation. This is the basic motivation for considering sophisticated molecular solvation theories in the context of ET applications.

Molecular level solvent models

The linearized MD scheme

The general analysis from the section "The linear response approach in the functional space" can be implemented for molecular computations based on the statistical mechanics treatment in terms of the Kirkwood formula for the response kernel $K(r,r')$ [57, 58]:

$$K(r,r') = -\frac{1}{k_B T}\left\langle \left(\tilde{\Phi}(r) - \Phi(r)\right)\left(\tilde{\Phi}(r') - \Phi(r')\right)\right\rangle_{\rho,T} \tag{22}$$

The response field $\tilde{\Phi}(r)$ is created in the solute region by an instantaneous solvent configuration (see Fig. 4); $\Phi(r) = \left\langle \tilde{\Phi}(r)\right\rangle_{\rho,T}$ is the average field. The average $\langle \ldots \rangle_{\rho,T}$ is performed in the external field created by the solute charge distribution ρ at temperature T.

It was found, however [13], that a straightforward simulation of Eq. 22 is inefficient. Simulations of average fields $\Phi_a(r)$ equilibrated to given charges $\rho_a(r)$ proved to be more convenient. By this means the equilibrium free energy is available as

$$\Delta F_a = \frac{1}{2}\int d^3 r \Phi_a(r)\rho_a(r) = \frac{1}{2}\left\langle \rho_a|\hat{K}|\rho_a\right\rangle \tag{23}$$

Cross terms (see Eq. 14), namely

$$-T_{ab} = \left\langle \rho_a|\hat{K}|\rho_b\right\rangle \tag{24}$$

are also available after $\Phi_a = \hat{K}\rho_a$ is calculated. Therefore, the method used for computation of the reorganization matrix is established.

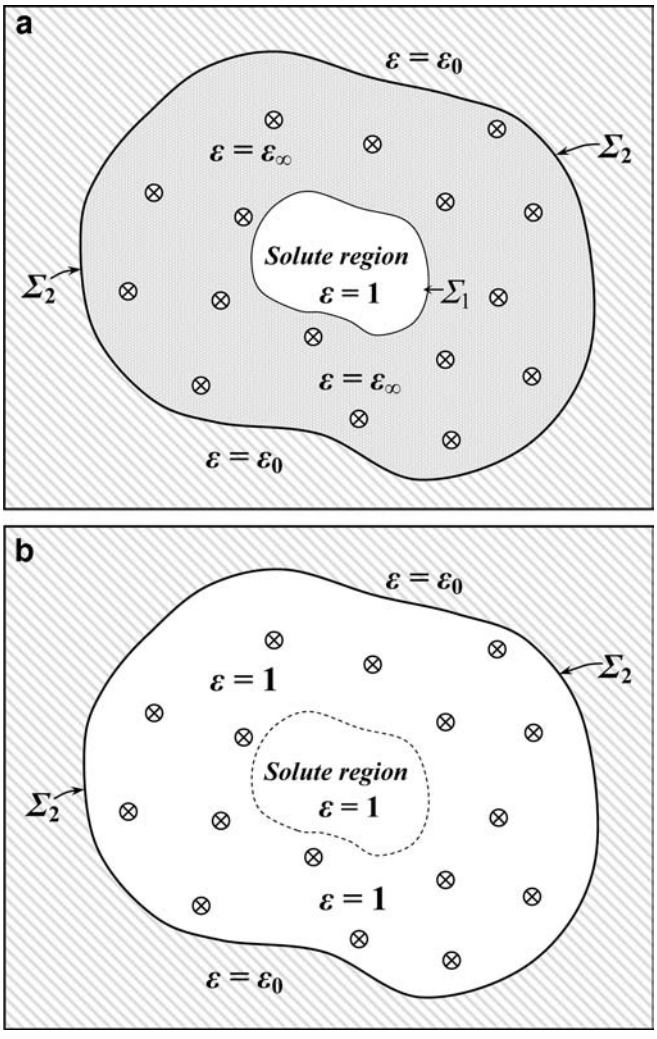

Fig. 4. Schemes of molecular/continuum solvent models. The solute charge density is confined within the solute region. Explicit solvent particles (crossed circles) fill the intermediate region. **a** MD/FRCM: the solute and intermediate regions have different dielectric permittivities ($\varepsilon = 1$ and $\varepsilon = \varepsilon_\infty$); **b** MD/PCM: the same $\varepsilon = 1$ for both solute and intermediate regions (surface Σ_1 is absent)

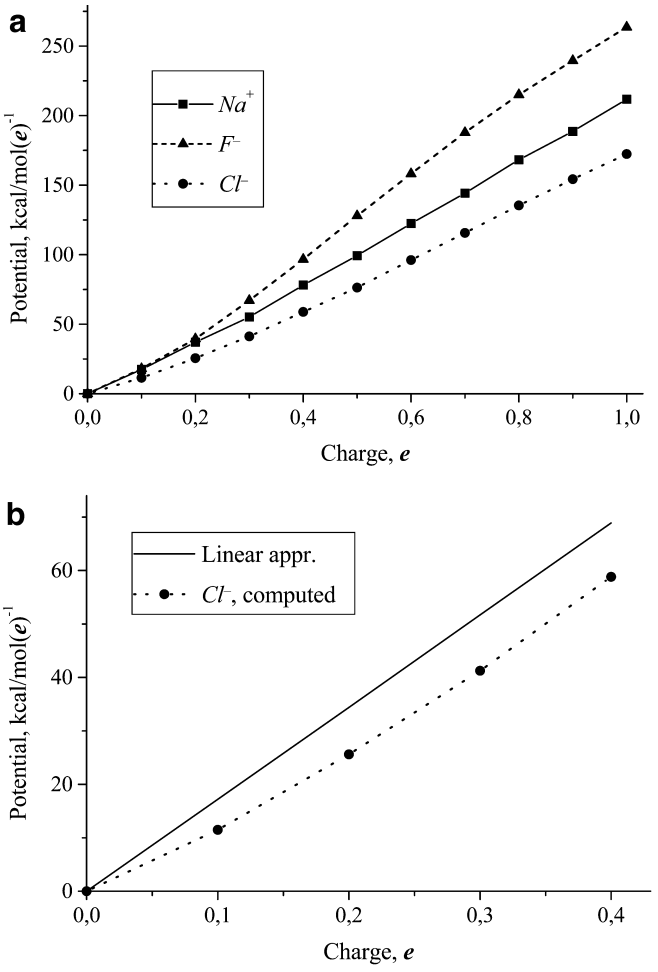

Fig. 5. Nonlinear effects in monoatomic ions. The average potential $\Phi(r = 0)$ calculated for variable charge Q, e denotes the electronic charge. **a** Na^+, F^- and Cl^- in water when Q changes from 0 to $+1e$; **b** Cl^- in water when Q changes from 0 to $+0.4e$ (dotted line). Solid line corresponds to the linear approximation

We see from Eq. 22 that $K(r,r')$ is, generally, ρ-dependent. Strictly speaking, one should change $\hat{K}$ to $\hat{K}_a$ in Eqs. 22, 23 and 24. The corresponding nonlinear effect can be estimated by studying the change of Φ during the so-called charging process (when ρ is varied from zero to the final value). For monatomic singly-charged ions we have to change the charge Q in the range $0 < |Q| < 1$; in this simple case it suffices to simulate $K(0,0) = \Phi(r = 0)$ as a function of $|Q|$ (where $r = 0$ is the position of the ion). The results shown in Fig. 5 correspond to a 3%, 4% and 7% nonlinearity correction in the free solvation energy for Na^+, F^-, and Cl^-, respectively, in water solvent [13].

There are two sources responsible for the nonlinear behavior. The first one is the solvent structure formation in the close vicinity of a solute observed in weak electric fields (small $|Q|$ values) [14, 15]. The most remarkable observation is that $\Phi \neq 0$ when $Q = 0$. The magnitude of this effect is not quite clear (see the discussions in [59, 60]). It seems to disappear in stronger solute fields where the linearity is regenerated. This explains naturally why the nonlinearity for F^- (smaller ion with stronger field) is less than for Cl^- (larger ion with a weaker field). At least partly, this effect can be imitated, within a linear theory, by introducing the field shift $\bar{\Phi}(Q)$ (see earlier section on "The linear response approach in the functional space"), which does not vanish when $Q = 0$ at equilibrium. This shift should be attributed to the interference of Coulomb and van der Waals effects revealed when Coulomb forces are weak.

Another nonlinear effect arises as a dependence of the response kernel on the sign of the charge Q. For monatomic ions, the response kernel is different for cations and anions with the same Lennard Jones (LJ) parameters. For monatomic ions in water $\frac{\partial \Phi}{\partial Q} = K(0,0)$ changes by $\sim$30% when the sign of the charge is changed [13, 14, 16]. This asymmetry finds its

explanation in terms of the asymmetry of charge distributions of solvent particles.

The last effect can be formally included in the linearization scheme by allowing the Q-dependence of kernel $K(r,r')$. As shown below, this sort of change becomes much more visible in the context of studying reorganization rather than equilibrium solvation energies.

Separation of the inertial response

The inertialess response field is created due to a polarization of the solvent electrons by the solute charge. Its consistent treatment, therefore, implies that polarizable solvent models must be implemented in computations. The pertaining techniques have been developing during the last decade [61, 62, 63, 64, 65, 66, 67, 68, 69, 70, 71 and references therein]. They treat electronic polarization at classical mechanical level, which is legitimate, due to the large distinction of electronic and nuclear timescales, provided only its average effect on the inertial nuclear dynamics is of main interest. Full polarizable molecular level algorithms require much more computational effort than the standard nonpolarizable simulation schemes usually applied. Polarizable methods provide total polarization response as an output result, but the problem of an extraction of its inertialess part can be resolved within this technique [70, 71].

Several molecular level computations of ET reorganization energies have been reported [72, 73, 74, 75, 76, 77,78, 79, 80]. They always encounter a problem of a consistent separation of electronic (inertialess) polarization. This problem was successfully solved in simple continuum ET theories [1, 2, 3, 4, 81] by introducing the so-called Pekar factor $(1/\varepsilon_\infty - 1/\varepsilon_0)$, where ε_∞ and ε_0 are optical and static dielectric constants of a polar medium, see Eq. 21. A quantity of this sort cannot naturally appear in a molecular simulation neglecting the electronic structure of solvent particles. Having been intensively discussed in the recent literature, the remedy to this serious deficiency of microscopic models was in some cases, with slight variations, reduced to a straightforward scaling of the computational results. Specifically, it was proposed to scale reorganization free energies by the ratio of the polarizable (including ε_∞) and nonpolarizable (setting $\varepsilon_\infty = 1$) Pekar factors [74, 75] (see also related discussion in [72, 73, 82, 83]). However, when applied to decoupling the electronic and nuclear response fields of a solvent in the presence of a charged nonspherical solute, such an approach seems to have no solid basis. Suggesting an alternative point of view, the present work circumvents this ad hoc postulate. According to the approach outlined below, a nonpolarizable simulation based on suitably scaled atomic point charges, and associated with the response of heavy particles (which promote the inertial polarization) directly yields the inertial part of the solvation free energy. The complementary inertialess part (the electronic response to the field of a solute charge), which constitutes an essential fraction of the total response, is estimated within a continuum approach and added to the inertial result extracted from a microscopic simulation. In this way, the basic idea borrowed from the continuum ET theory [1, 2, 3, 4, 81] is implemented in the context of a combined molecular/continuum model of polar solvation.

This consideration gives rise to the following model [84]. Explicit solvent particles with mean dipoles $\bar{\mu}$ and associated mean point charges assigned to the selected sites of the solvent molecules, $\bar{q}_v (\sum_v \bar{q}_v = 0)$, are immersed in a medium with $\varepsilon = \varepsilon_\infty$. The solute particle with charges q_i (taken as nonpolarizable in the present study) can be added to this picture, as shown in Fig. 4a. It is placed at the center of the MD cell. Nonelectrostatic intermolecular forces are described in terms of pairwise LJ potentials. In order to treat electrostatic forces we represent the solvent charge density ρ_{slv} as:

$$\rho_{\mathrm{slv}} = \sum_v \bar{q}_v \delta(r - r_v) \tag{25}$$

The electronic continuum is bounded from inside by the solute region with $\varepsilon = 1$ occupying volume V_0, which is surrounded by boundary surface Σ_1 (Fig. 4a). The solute charge density ρ_{slt} is represented analogously as:

$$\rho_{\mathrm{slt}} = \sum_i q_i \delta(r - r_i) \tag{26}$$

In order to properly treat long-range electrostatic interactions we introduce the external continuum with static dielectric constant $\varepsilon = \varepsilon_0$. This continuum fills the volume V_2 outside boundary surface Σ_2. The explicit solvent region with $\varepsilon = \varepsilon_\infty$ and volume V_1 is confined between surfaces Σ_1 and Σ_2. A complication of the model, due to the introduction of the external region, is motivated by a purely technical reason of getting a reasonably convergent computation.

A special comment is required about the nature of solvent charges $\bar{q}_v$. According to the above formulation, they represent effective charge distributions of solvent particles in the bulk solvent. That is to say, the charges q_v of isolated (gas phase) molecules are surrounded by a cloud of electronic polarization that transforms them into $\bar{q}_v$. The "dressed" average charges $\bar{q}_v$ can be borrowed from polarizable simulations of bulk solvent. The main assumption of the present model introduces scaled electrostatic interactions:

$$\underset{\text{(solvent/solvent)}}{\frac{\bar{q}_\mu \bar{q}_v}{\varepsilon_\infty r_{\mu v}}} \quad \text{and} \quad \underset{\text{(solute/solvent)}}{\frac{q_i \bar{q}_v}{\varepsilon_\infty r_{iv}}} \tag{27}$$

where $r_{\mu v} = |r_\mu - r_v|$ and $r_{iv} = |r_i - r_v|$.

On the other hand, if one addresses nonpolarizable simulations of the bulk solvent, the electrostatic interactions are represented as

$$\frac{q_\mu^{\text{eff}} q_\nu^{\text{eff}}}{r_{\mu\nu}} \tag{28}$$

where $q_{\mu,\nu}^{\text{eff}}$ represents effective solvent charges fitted according to a particular nonpolarizable scheme. These two pictures can be coordinated by assuming

$$q_\mu^{\text{eff}} = \frac{\bar{q}_\mu}{\sqrt{\varepsilon_\infty}} \tag{29}$$

Therefore, one can perform a standard nonpolarizable simulation in the presence of the solute using interaction laws (Eq. 27), provided the dressed charges $\bar{q}_\nu$ are connected by Eq. 29 to the effective charges q_ν^{eff}, corresponding, say, to the SPC water model.

The reasoning outlined above can be illustrated as follows. The effective dipole moment of the SPC water is $\mu^{\text{eff}} = 2.27D$ [85]. According to Eq. 29, the dipole moment of dressed bulk water molecules is $\bar{\mu} = \mu^{\text{eff}}\sqrt{\varepsilon_\infty}$. For $\varepsilon_\infty = 1.8$ this gives $\bar{\mu} = 3.05D$. This value is in good agreement with recent estimates based on calculation with polarizable models ($2.95 \pm 0.2D$ [86, 87, 88, 89]) and experiment ($2.9 \pm 0.6D$ [90]), which supports the renormalization of charges as suggested by Eq. 29 and provides a link between the present approach and conventional nonpolarizable solvent models.

To summarize, the electrostatic forces between explicit solute and solvent charges q_i and $\bar{q}_\nu$ as well as between solvent charges $\bar{q}_\mu$, $\bar{q}_\nu$, are scaled by the factor $1/\varepsilon_\infty$. In combination with van der Waals (LJ) forces they form the effective force field applied for a nonpolarizable MD simulation producing the equilibrium ensemble of solvent particles. Such a simplistic treatment of electrostatic interactions (neglecting the presence of the solute region V_0 with $\varepsilon = 1$, as in Fig. 4a) seems legitimate because the LJ forces due to the solute provide the excluded volume effect so that solvent particles cannot penetrate into V_0. Computations confirm this guess [84].

The combination of charge distributions (25) and (26) and the dielectric continuum scheme represented by Fig. 4a leads to the following expression for the average medium response field:

$$\Phi(r) = \Phi_{\text{d}}(r) + \Phi_{\text{c}}(r) \tag{30}$$

The first term, called direct field, represents the electrostatic response due to explicit solvent particles contained in volume V_1:

$$\Phi_{\text{d}}(r) = \left\langle \sum_\nu \frac{\bar{q}_\nu}{\varepsilon_\infty} \frac{1}{|r - r_\nu|} \right\rangle_{\rho,T} \tag{31}$$

Here the average is performed over the equilibrium ensemble found in the MD simulation described above. The second term, called the continuum field, is the response of the dielectric continuum, contained in both volumes V_1 and V_2, to the electric field created by the solute charge distribution (26). It is easy to see that its computation can be performed in terms of the FRCM procedure described above in the section "Breakdown of the PCM approach and the advanced continuum theory". The only modification assumes that the intermediate layer with volume V_1 is much larger than in the conventional purely continuum scheme; in the present procedure the external boundary surface Σ_2 is shifted as far as possible away from the solute region in order to properly represent the molecular structure of the solvent. We have omitted in Eq. 30 small interference terms arising from interactions of the explicit solvent charges (Eq. 25) with the continuum. They were shown to be negligible according to test computations [84].

The result (30) represents the total medium response. In order to separate out its inertial part we simply repeat the FRCM prescription:

$$\Phi_{\text{in}}(r) = \Phi_{\text{d}}(r) + \Phi_{\text{c}}(r) - \Phi_\infty(r) \tag{32}$$

where $\Phi_\infty(r)$ is found in a PCM computation in which $\varepsilon = \varepsilon_\infty$ outside the surface Σ_1 bounding the solute region covering the whole external space.

First results from MD/FRCM computations

The computational scheme described in the section on the "Separation of the inertial response" is called MD/FRCM. It was applied for calculations of equilibrium solvation energies for a large number of polyatomic ions. The structure and charge distribution of the given ion was computed using the restricted Hartree-Fock level with the 6–31G** basis set. The standard LJ parameters, that were not specially calibrated to fit the solvation energies, were used in MD simulations [91]. Water (the SPC model [85]) was considered as a solvent. The computations showed [92] that the MD/FRCM scheme works satisfactorily for nitrogen cations in the frame of a standard parameterization and can be further improved for oxygen ions by tuning solute/solvent LJ parameters. The calculated relative change of the energies in families of similar cations (ammonium-type or oxonium-type cations) fits the experimental trends.

A more conventional simple computational scheme is illustrated in Fig. 4b. It counts the response field of explicit solvent particles in a straightforward manner by performing a standard nonpolarizable MD simulation in the region bounded by the external surface Σ_2. Outside this surface the solvent is modeled as a continuum with $\varepsilon = \varepsilon_0$. Similar to MD/FRCM, this approximation is invoked only for a technical reason in order to keep the MD run to a reasonable computational cost. The response field has the form

$$\Phi(r) = \left\langle \sum \frac{q_v^{\text{eff}}}{|r - r_v|} \right\rangle_{\rho,T} + \Phi_{\text{PCM}}(r) \tag{33}$$

The first term is a counterpart of the direct term (31) arising in the MD/FRCM. Its averaging is performed in the field created by the solute and explicit solvent particles. Contrary to Eq. 31, no scaling of solvent charges is required both in the averaging procedure and at the MD simulation stage. Obtained under such conditions, this term exactly equals $\varepsilon_\infty \Phi_d$ [84].

The second term in Eq. 33 is the continuum response field available by a standard PCM procedure. Solvent charges are neglected during this computation because the contribution due to their polarization of the external continuum proved to be negligible. The free energy computations using response field (33) will be denoted as MD/PCM.

The equilibrium solvation free energies obtained in terms of MD/FRCM were shown [92] to be slightly better (compared to the experiment) than those resulting from MD/PCM. More important is the advantage that the separation of the inertial free energy contribution is naturally included in the MD/FRCM, whereas MD/PCM provides no consistent prescription for this purpose. The only available way of doing this is empirical scaling by means of the Pekar factor $(1/\varepsilon_\infty - 1/\varepsilon_0)$ [72, 73, 74, 75, 82, 83]. Table 2 compares the results of the two methods for a series of polyatomic ions in water. The discrepancy is sometimes significant but not impressive. A much larger deviation was observed [92] in the test using tetrahydrofuran (THF) solvent with $\varepsilon_\infty = 1.97$ and $\varepsilon_0 = 7.58$. The Pekar factor scaling, being more or less acceptable for water, becomes invalid for the case of THF. Direct contribution to the solvation free energy (ΔF_d) is also shown in Table 2. It could be an adequate measure of the inertial contribution provided the complementary continuum field component in Eq. 30 is negligible; in other words the external surface Σ_2 is shifted extremely far away from the solute region. This is not so in actual computations.

Table 2. The ΔF values computed via the MD/FRCM model using ab initio RHF charges, the inertial component of solvation energy ΔF_{in}, and the direct part ΔF_d[a]. The inertial component calculated using the Pekar/Born ratio[b] is also given. The units are Kcal/mol

Ion	ΔF	ΔF_d[a]	ΔF_{in}	
			MD/FRCM	Pekar/Born ratio[b]
NH_4+	−85.8	−34.1	−39.7	−47.2
$MeNH_3+$	−74.1	−28.6	−34.4	−40.7
Me_2NH_2+	−65.7	−25.7	−31.4	−36.1
Me_3NH+	−59.7	−22.9	−28.6	−32.8
$PhNH_3+$	−65.1	−24.6	−30.4	−35.8
C_5H_5NH+	57.9	−22.2	−27.9	−31.8
$MeOH_2+$	−87.6	−40.0	−45.8	−48.2
$EtOH_2+$	−83.8	−39.0	−44.7	−46.1
MeO^-	−106.3	−51.9	−57.7	−58.4
PhO^-	−72.6	−31.6	−37.5	−39.9

[a] The contribution due to the direct response field, Eq. 31;

[b] The scaling factor is $\left(\frac{1}{\varepsilon_\infty} - \frac{1}{\varepsilon_0}\right) \Big/ \left(1 - \frac{1}{\varepsilon_0}\right)$

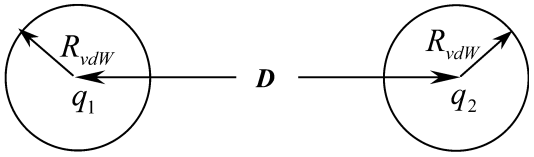

In terms of MD/FRCM, we can fully apply the methodology for a computation of charge transfer reorganization energies developed in the section "The reorganization energy". It was implemented for the model two-site dipolar system in SPC water solvent.

In this scheme D is the intersite separation, q_1 and q_2 are site charges and R_{vdW} are van der Waals radii defined in terms of site Lennard Jones parameters.

We studied three different processes, represented schematically as:

a. hole transfer: (1, 0) → (0, 1)
b. electron transfer: (0, −1) → (−1, 0)
c. charge separation: (0, 0) → (−1, +1)

The numbers in brackets denote charge occupations of sites 1 and 2.

The standard linear-response approach holds with high accuracy for every particular reaction but it proved to be significantly violated when reorganization energies of different reactions were compared. The computations are listed in Table 3.

This new result has a purely molecular origin and is absent within a conventional continuum solvent model. It can be explained in terms of the ρ-dependence of the kernel of the response operator $\hat{K}$ (Eqs. (1) and (22)).

More specifically, the continuum approach suggests Eq. 13 as a common expression for all three reactions a–c. Computations in Table 3, based on ρ-dependent response operators $\hat{K}_I$ and $\hat{K}_{II}$ that represent initial (I) and final (II) ET states, were obtained as half-sums of corresponding reorganization energies λ_I and λ_{II} in accord with Eq. 11.

The observed discrepancy in reorganization energies for the three reactions is significant. This effect is probably exaggerated in the present treatment due to the oversimplified solute model. We assumed the same

Table 3. Reorganization energies λ for reactions (a) (c)[84]

Type of reaction	λ (Kcal/mol)	
	$D = 10$ Å	$D = 5$ Å
(a)	52.8	32.3
(b)	78.0	59.0
(c)	64.3	45.2

LJ parameters for both dumbbell sites, irrespective of the charges. Proper parameterization of solute/solvent LJ forces for realistic chemical systems may well reduce the magnitude of the observed discrepancies. The finding that the effective radius of an anionic atomic site is often larger than for the isoelectronic cationic counterpart [14, 16] gives some support for this expectation.

Conclusions

Computations of solvent reorganization energies λ are important, not only in the context of ET applications, but also as an example of treating an essentially non-equilibrium solvation phenomenon by means of methodologies available in recent theoretical chemistry. Standard purely electrostatic solvation models should be refined in order to account properly for this sort of phenomenon. Advanced continuum models, like FRCM, are sufficient for the limited purpose of considering trends in λ values for a series of ET solutes in a single polar solvent. More subtle effects, associated with combined translational and rotational motion of solvent particles, can only be understood at a truly molecular level of solvent description. They are usually revealed in solutes of low polarity where purely electrostatic effects are suppressed significantly. Being treated in terms of the MSA model, assuming spherical shapes for solute particles, the molecular level approach can properly describe trends in solvation effects produced by a number of solvents for a given single solute [28, 29, 42, 43, 44, 45]. The further refinement of the molecular approach, free of such limitations, involves computer simulation technologies.

Molecular level computations have revealed peculiar nonlinear effects that can considerably modify the traditional concepts, based on the linear response approximation, that underlie the recently accepted theory of ET reactions. Currently, it is not clear to what extent these observations, made for oversimplified model objects, may be important in the world of real chemical ET systems. Further studies in this direction are required. Therefore, the theme discussed in the present article seems to lie on the frontier of important applications of recent theoretical chemistry and biology. Its further development is expected to bring interesting results.

Acknowledgements. This article is dedicated to the anniversary of Professor Jacopo Tomasi, who has made a significant contribution to the solvation theory.The authors are indebted to I. V. Rostov and M. V. Vener, active participants in the research described in this article. The important contribution of G. E. Chudinov at the earlier stage of this work should also be emphasized.IVL and MVB thank the Russian Foundation of Fundamental Research (Project Nos. 02-03-33049 and 00-15-97295) and the Civilian Research and Development Foundation (CRDF) for the Independent States of the Former Soviet Union (Award No RC2-2209) for financial support. The research at the Karpov Institute was supported in part by the International Association for the Promotion and Cooperation with Scientists from the New Independent States of the former Soviet Union (project INTAS-RFBR IR-97-620). The research at Brookhaven National Laboratory was carried out under contract DE-AC02-98CH10886 with the U.S. Department of Energy and supported by its Division of Chemical Sciences, Office of Basic Energy Sciences.

References

1. Marcus RA (1956) J Chem Phys 24:966
2. Marcus RA (1965) J Chem Phys 43:679
3. Levich VG, Dogonadze RR (1959) Dokl Akad Nauk SSSR + 124:123
4. Ulstrup J (1979) Charge transfer processes in condensed media. Springer, Berlin Heidelberg New York
5. Miertus S, Scrocco E, Tomasi J (1981) Chem Phys 55:117
6. Tomasi J (1995) J Comput Chem 16:1449
7. Tomasi J, Persico M (1994) Chem Rev 94:2027
8. Basilevsky MV, Chudinov GE, Newton MD (1994) Chem Phys 179:263
9. Liu Y-P, Newton MD (1995) J Phys Chem 99:12382
10. Basilevsky MV, Chudinov GE, Rostov IV, Liu Y-P, Newton MD (1996) J Mol Struc–Theochem 371:191
11. Basilevsky MV, Rostov IV, Newton MD (1998) Chem Phys 232:189
12. Newton MD, Rostov IV, Basilevsky MV (1998) Chem Phys 232:201
13. Vener MV, Leontyev IV, Dyakov YuA, Basilevsky MV, Newton MD (2002) J Phys Chem B 106:13078
14. Hummer G, Pratt LR, Garcia AE (1996) J Phys Chem 100:1206
15. Åqvist J, Hansson T (1996) J Phys Chem 100:9512
16. Hummer G, Pratt LR, Garcia AE (1997) J Amer Chem Soc 119:8523
17. Marcus RA, Sutin N (1985) Biochem Biophys Acta 811:265
18. Newton MD (1999) Adv Chem Phys 106:303
19. Basilevsky MV, Chudinov GE (1991) Chem Phys 157:327
20. Basilevsky MV, Chudinov GE (1991) Chem Phys 157:345
21. Kurnikov IV, Zusman LD, Kurnikova MG, Farid RS, Beratan DN (1997) J Am Chem Soc 119:5690
22. Kumar K, Kurnikov IV, Beratan DN, Waldeck DH, Zimmt MB (1998) J Phys Chem A 102:5529
23. Closs GL, Calcaterra LT, Green NJ, Penfield KW, Miller JR (1986) J Phys Chem 90:3673
24. Miller JR, Paulson BP, Bal R, Closs GL (1995) J Phys Chem 99:6923
25. Closs GL, Miller JR (1988) Science 240:440
26. Chudinov GE, Napolov DV, Basilevsky MV (1992) Chem Phys 160:41
27. Rostov IV, Basilevsky MV, Newton MD (1999) In: Pratt LR, Hummer G (eds) Simulation of electrostatic interactions in solution. AIP, New York, p 331
28. Vath P, Zimmt MB, Matyushov DV, Voth GA (1999) J Phys Chem B 103:9130
29. Vath P, Zimmt MB (2000) J Phys Chem A 104:2626
30. Reynolds L, Gardecki JA, Frankland SJV, Horng ML, Maroncelli M (1996) J Phys Chem 100:10337
31. Chandra A, Bagchi B (1989) J Phys Chem 93:6996
32. Bagchi B, Chandra A (1991) Adv Chem Phys 80:1
33. Matyushov DV (1993) Chem Phys 174:199
34. Matyushov DV (1996) Chem Phys 251:1
35. Matyushov DV, Schmid R (1994) J Phys Chem 98:5152
36. Jeon J, Kim HJ (2000) J Phys Chem A 104:9812
37. Jeon J, Kim HJ (2001) J Solution Chem 30:849
38. Dorairaj S, Kim HJ (2002) J Phys Chem A 106:2322
39. Wertheim MS (1971) J Chem Phys 55:4291
40. Chan DYC, Mitchell DJ, Ninham BW (1979) J Chem Phys 70:2946
41. Blum L, Fawcett WR (1992) J Phys Chem 96:408
42. Matyushov DV (1996) Chem Phys 211:47
43. Matyushov DV, Voth GA (1999) J Chem Phys 111:3630
44. Read I, Napper A, Zimmt MB, Waldeck DH (2000) J Phys Chem A 104:9385
45. Napper AM, Read I, Kaplan R, Zimmt MB, Waldeck DH (2002) J Phys Chem A 106:5288

46. Dogonadze RR, Kornyshev AA (1974) J Chem Soc Farad T 2 70:1121
47. Kornyshev AA (1985) In: Dogonadze R, Kalman E, Kornyshev AA, Ulstrup J (eds) The chemical physics of solvation, part A. Elsevier, Amsterdam, p 77
48. Basilevsky MV, Parsons DF (1988) J Chem Phys 108:9107
49. Chandra A, Bagchi B (1989) J Chem Phys 90:1832
50. Atard P, Wei D, Patey GN (1990) Chem Phys Lett 172:69
51. Fonseca T, Ladanyi BM (1990) J Chem Phys 93:8148
52. Fonseca T, Ladanyi BM (1991) J Phys Chem 95:2116
53. Raineri FO, Zhou Y, Friedman HL (1991) Chem Phys 152:201
54. Raineri FO, Resat H, Friedman HL (1992) J Chem Phys 96:3068
55. Bopp PA, Komyshev AA, Sutmann G (1996) Phys Rev Lett 76:1280
56. Kornyshev AA, Leikin S, Sutmann G (1997) Electrochim Acta 42:849
57. Kirkwood JG (1939) J Chem Phys 7:39
58. Kubo K, Toda M, Hatshisume N (1985) Statistical Physics II. Springer, Berlin Heidelberg New York
59. Hummer G, Pratt LR, Garcia AE, Berne BJ, Rick SW (1997) J Phys Chem B 101:3017
60. Åqvist J, Hansson T (1988) J Phys Chem B 102:3837
61. Rullman JAC, van Duijnen PT (1988) Mol Phys 63:451
62. Ahlström P, Wallqvist A, Engström S, Jönsson B (1989) Mol Phys 68:563
63. Dang LX, Rice JE, Caldwell J, Kollman PA (1991) J Am Chem Soc 113:2481
64. Van Belle D, Froeyen M, Lippens G, Wodak SJ (1992) Mol Phys 77:239
65. Bursulaya BD, Kim HJ (1998) J Chem Phys 109:4911
66. Sprik M, Klein ML, Watanabe K (1990) J Phys Chem 94:6483
67. Rick SW, Stuart SJ, Berne BJ (1994) J Chem Phys 101:6141
68. Stuart SJ, Berne BJ (1996) J Phys Chem 100:11934
69. Rick, Berne BJ (1997) J Phys Chem B 101:10488
70. Berne JS, Bader BJ (1996) J Chem Phys 104:1293
71. Bader BJ, Cortis CM, Berne JS (1997) J Chem Phys 106:2372
72. Perng B-C, Newton MD, Raineri FO, Friedman HL (1996) J Chem Phys 104:7153
73. Perng B-C, Newton MD, Raineri FO, Friedman HL (1996) J Chem Phys 104:7177
74. Marchi M, Gehlen JN, Chandler D, Newton M (1993) J Am Chem Soc 115:4178
75. Ungar LW, Newton MD, Voth GA (1999) J Phys Chem B 103:7367
76. Ando K (1997) J Chem Phys 106:116
77. Ando K (2001) J Chem Phys 114:9040
78. Ando K (2001) J Chem Phys 114:9471
79. Ando K (2001) J Chem Phys 115:5228
80. Harting C, Kopera MTM (2001) J Chem Phys 115:8540
81. Pekar SI (1954) Untersuchungen über die electronentheorie der kristalle. Akademic Verlag, Berlin
82. Warshel A, Hwang J-K (1986) J Chem Phys 84:4938
83. Hwang J-K, Warshel A (1987) J Am Chem Soc 109:715
84. Leontyev IV, Vener MV, Rostov IV, Basilevsky MV, Newton MD (2003) J Chem Phys 119:8024
85. Berendsen HJC, Postma JPM, van Gunsteren WF, Hermans J (1981) In: Pullman B (ed) Intermolecular forces. D. Reidel, Dordrecht, p 331
86. Rick SW (2001) J Chem Phys 114:2276
87. Gulskaya AA, Kusalik PG (2002) J Chem Phys 117:5290
88. Silvestrelli PL, Parrinello M (1999) J. Chem. Phys 111:3572
89. Dang LX, Chang T-M (1997) J. Chem. Phys 106:8149
90. Badyal YS, Saboungi M-L, Price DL, Shastri SD, Haeffner DR, Soper AK (2000) J Chem Phys 112:9206
91. Van Gunsteren WF, Billeter SR, Eising AA, Hünenberger PH, Krüger P, Mark AE, Scott WRP, Tironi IG (1996) Biomolecular simulation: the GROMOS96 manual and user guide. vdf Hochschulverlag AG an der ETH Zürich and BIOMOS b.v., Zürich, Groningen
92. Vener MV, Leontyev IV, Basilevsky MV (2003) J Chem Phys 119:8038